

Synthesis of the first nanomagnetic particles with semicarbazide-based acidic ionic liquid tag: an efficient catalyst for the synthesis of 3,3'-(arylmethylene)bis(4-hydroxycoumarin) and 1-carbamato-alkyl-2-naphthol derivatives under mild and green conditions

Mohammad Ali Zolfigol*, Roya Ayazi-Nasrabadi and Saeed Baghery



Semicarbazide functionalized with chlorosulfonic acid on the surface of silica-coated magnetic nanoparticles, $\{Fe_3O_4@SiO_2@(CH_2)_3\text{Semicarbazide-SO}_3H/HCl\}$, as a novel magnetic Brønsted acid catalyst according to the aims of green chemistry was synthesized and fully characterized using Fourier transform infrared, UV-visible and energy-dispersive X-ray spectroscopies, X-ray diffraction, scanning electron, transmission electron and atomic force microscopies and thermogravimetric analysis. The capability and excellent activity of this nanoparticle catalyst were exhibited in the synthesis of two series of compounds with important biological activities, namely 3,3'-(arylmethylene)bis(4-hydroxycoumarin) and 1-carbamato-alkyl-2-naphthol derivatives, under mild, green and solvent-free conditions. To the best of our knowledge, this is the first study of the synthesis and application of $\{Fe_3O_4@SiO_2@(CH_2)_3\text{Semicarbazide-SO}_3H/HCl\}$ as Brønsted acid solid magnetic nanoparticles. Consequently the present study can open up a novel and promising intuition in the sequence of logical design, synthesis and applications of task-specific Brønsted acid magnetic nanoparticle catalyst with favourable properties as a full-fledged efficient material for sustainable approaches. Copyright © 2016 John Wiley & Sons, Ltd.

Additional supporting information may be found in the online version of this article at the publisher's web site.

Keywords: semicarbazide-based ionic liquid; nanomagnetic silica-coated Fe_3O_4 functionalized with ionic liquid; $\{Fe_3O_4@SiO_2@(CH_2)_3\text{Semicarbazide-SO}_3H/HCl\}$; 3,3'-(arylmethylene)bis(4-hydroxycoumarin); 1-carbamato-alkyl-2-naphthol; solvent-free

Introduction

Nowadays knowledge-based and rational design and synthesis of task-specific and biological-based catalysts are more in demand because catalytic systems have played an excellent role in pollution prevention in our environment.^[1] In this regard, a wide range of solid catalysts and their supported forms have been reported in the last few years for various chemical processes and have been reviewed extensively. Among the reported solid catalysts, solid acids have been also used widely for various organic functional group transformations.^[2]

The study of solid acid catalysis has been carried out broadly and it has had much influence on the improvement of both basic investigation and chemical industry, principally in the field of chemistry-based processes. More wide and quantitative investigation of the acidic property of solid materials is nowadays preferred to correlate this property with stability, catalytic activity, selectivity and high turnover number and frequency, and to clarify the nature of acid–base bifunctional catalysis.^[3] Heterogeneous catalysts have the advantage of easy separation from products without the necessity of washing. Also, recyclability and reusability of heterogeneous

catalysts are benefits over homogeneous ones.^[4] One method is the immobilization of a catalytic homogeneous tag on a nanomagnetic hybrid solid material, to convert it to a heterogeneous catalyst with homogeneous action in chemical-based processes.

Among the four types of magnetic nanoparticles (MNPs), i.e. metals, alloys, metal oxides and ferrites, iron oxides have attracted the most attention, because they can be produced easily via sedimentation and also they have stronger magnetic properties. While several improvements have been realized in the synthesis and application of MNPs, their consistency in the long term without aggregation or surface oxidation is still a concern.^[5–8]

In the well-known class of coumarin derivatives, dimeric coumarins (also named biscoumarins) are of particular interest. Biscoumarin derivatives occur naturally in a great number of plants and

* Correspondence to: M. A. Zolfigol, Department of Organic Chemistry, Faculty of Chemistry, Bu-Ali Sina University, Hamedan 6517838683, Iran. E-mail: zolfi@basu.ac.ir

Department of Organic Chemistry, Faculty of Chemistry, Bu-Ali Sina University, Hamedan 6517838683, Iran

microorganisms.^[9,10] They are frequently biologically active^[11–14] and many of them have been confirmed in view of therapeutic usage,^[15] as anti-inflammatory,^[16] anticoagulant,^[17,18] cardiovascular,^[19] antimicrobial^[20] and anti-proliferative factors.^[21–23] Lately, numerous approaches have been studied for the preparation of biscoumarin derivatives via reactions between 4-hydroxycoumarin and numerous aldehydes.^[24–29]

Correspondingly, amidoalkyl naphthol derivatives are of significance as they can be effortlessly converted to biologically active compounds, through amide hydrolysis reaction. Hypotensive and bradycardiac properties have been reported for this type of compounds.^[30–32] Amidoalkyl naphthols can also be changed to 1,3-oxazine derivatives.^[33] 1,3-Oxazines have potentially different biological activities including antihypertensive, antimalarial, antitumor, anticonvulsant, antianginal, antipsychotic, analgesic, antibiotic and antirheumatic properties.^[34–42] Several Lewis and Brønsted acids have been applied to catalyse this transformation, such as [Msim]Cl, [Dsim]Cl, [Msim]AlCl₄,^[43] [Et₃N–SO₃H]Cl,^[44] nano-S (S8-NP),^[45] saccharin sulfonic acid,^[46] [2-MPyH]OTf,^[47] {[HMIM]C(CN)₃},^[48] cation-exchanged resins,^[49] sulfamic acid/ultrasound,^[50] HClO₄/SiO₂^[51] and H₃PW₁₂O₄₀.^[52]

In continuation of our studies of the synthesis and application of solid acids,^[53] inorganic acidic salts,^[54] nanomagnetic catalysts^[55] and knowledge-based improvement of task-specific ionic liquids,^[56] it was found that favourable structural diversity of ionic liquids with outstanding properties could be attained via design, synthesis and application of novel cationic cores with appropriate anionic counterparts. With this target, it was decided to join all of these investigation areas to the design, synthesis and applications of semicarbazide functionalized with chlorosulfonic acid on the surface of silica-coated MNPs, namely {Fe₃O₄@SiO₂-(CH₂)₃Semicarbazide-SO₃H/HCl}, as a green and mild heterogeneous catalyst for the synthesis of 3,3'-(arylmethylene)bis(4-hydroxycoumarin) and 1-carbamato-alkyl-2-naphthol derivatives under solvent-free conditions (Scheme 1).

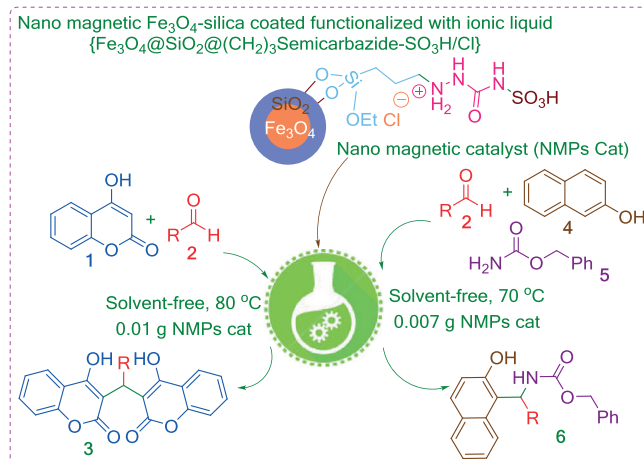
Results and discussion

Characterization of novel {Fe₃O₄@SiO₂-(CH₂)₃Semicarbazide-SO₃H/HCl} catalyst

Recently, Gu and co-workers reported a sulfonyl-containing ammonium-based Brønsted acid ionic liquid as an efficient liquid heterogeneous catalyst for the synthesis of a wide range of organic compounds under solvent-free conditions.^[57] In this way, nanospherical silica with imidazole linker and sulfonic acid tag for various multicomponent reactions^[58] has also been reported by our research group. Herein, we report novel core-shell nanomagnetic silica coated with semicarbazide spacer and sulfonic acid tag.

{Fe₃O₄@SiO₂-(CH₂)₃Semicarbazide-SO₃H/HCl} as a novel, green and task-specific catalyst was synthesized and fully characterized using Fourier transform infrared (FT-IR), UV-visible and energy-dispersive X-ray (EDX) spectroscopies, thermogravimetric analysis (TGA), X-ray diffraction (XRD), scanning electron microscopy (SEM), transmission electron microscopy (TEM) and atomic force microscopy (AFM). Generally, with the addition of substance in each synthesis step, FT-IR, EDX and UV-visible spectra, TGA and XRD patterns confirm the synthesis of pro-catalyst. Changes in any of these analyses indicate that the material is added in each synthesis step.

FT-IR spectroscopy was employed to compare the synthesized blank Fe₃O₄ MNPs, Fe₃O₄@SiO₂ core-shell MNPs and the other core-shell surface-modified models (Fig. 1). The FT-IR spectrum of



Scheme 1. The synthesis of 3,3'-(arylmethylene)bis(4-hydroxycoumarin) and 1-carbamato-alkyl-2-naphthol derivatives using novel semicarbazide functionalized with chlorosulfonic acid on the surface of silica-coated MNPs, i.e. {Fe₃O₄@SiO₂-(CH₂)₃Semicarbazide-SO₃H/HCl}, as a green and mild catalyst.

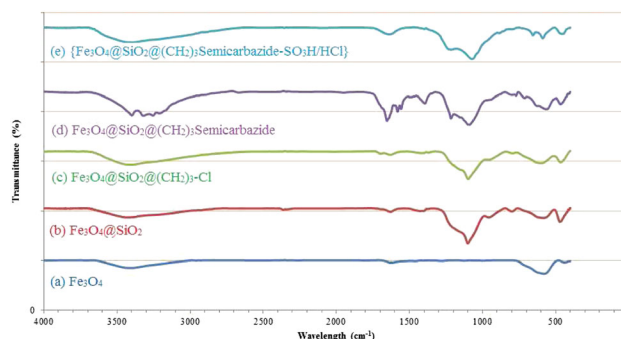


Figure 1. FT-IR spectra: (a) Fe₃O₄; (b) Fe₃O₄@SiO₂; (c) Fe₃O₄@SiO₂-(CH₂)₃-Cl; (d) Fe₃O₄@SiO₂-(CH₂)₃Semicarbazide; (e) {Fe₃O₄@SiO₂-(CH₂)₃Semicarbazide-SO₃H/HCl}.

the bare Fe₃O₄ MNPs shows a characteristic absorption peak of Fe O bond at about 580 cm⁻¹. The absorption peaks of the silica shell in the Fe₃O₄@SiO₂ core-shell MNPs at about 1100 and 798 cm⁻¹ are related to the antisymmetric and symmetric stretching vibrations of Si O Si bond in oxygen-silica tetrahedra, respectively. Correspondingly, the absorption peak of the Fe₃O₄@SiO₂-(CH₂)₃ core-shell MNPs at 2930 cm⁻¹ is linked to the stretching vibration of C H groups. The absorption peak at 1632 cm⁻¹ is also linked to the stretching vibration of C O bond of semicarbazide group. Furthermore, the absorption band at 3320 cm⁻¹ corresponds to stretching vibration of OH in the SO₃H group and the peak at 1177 cm⁻¹ is related to vibrational modes of O SO₂ bonds. The absorption associated with S O bond vibration appears at 1059 cm⁻¹.

UV-visible spectroscopy was another technique applied for proving the structure of {Fe₃O₄@SiO₂-(CH₂)₃Semicarbazide-SO₃H/HCl} as a MNP catalyst. This analysis was used to compare alterations in the various steps of catalyst synthesis. Hence, it was found that there are differences in absorption maxima among catalyst structure {Fe₃O₄@SiO₂-(CH₂)₃Semicarbazide-SO₃H/HCl} and other structures, and this emphasizes the synthesis of this compound. We are able to identify the presence of an additional moiety on the chief structure of MNPs, especially at λ = 272 nm (Fig. 2). These step-by-step changes in the UV-visible spectra represent the preparation of the MNP catalyst. The intensity of absorption at λ = 272 nm

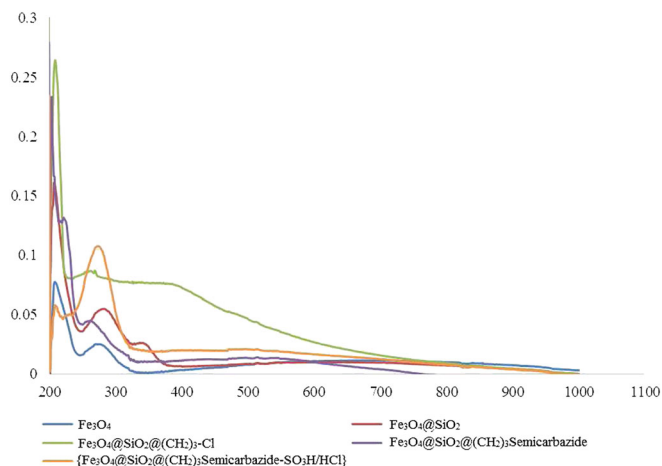


Figure 2. UV-visible absorption curves of $\{\text{Fe}_3\text{O}_4@\text{SiO}_2@(\text{CH}_2)_3\text{Semicarbazide-SO}_3\text{H/HCl}\}$ as a MNP catalyst.

changes during the synthesis of the MNP catalyst in each stage. Moreover, band-gap energy (E_{bg}) is calculated on the basis of the maximum absorption band of the catalyst and is determined as 4.559 eV, using the equation E_{bg} (eV) = $1240/\lambda$ (where E_{bg} is the band-gap energy and λ_{max} is the absorption wavelength (ca 272 nm) of the MNP catalyst. No additional peaks linked with impurities and structural imperfections are seen in the spectrum, which indicates that the MNP catalyst had been prepared. The samples for UV-visible spectral investigation were prepared in ethanol solvent and a concentration of 0.1 g of MNP catalyst was studied (via dispersing process).

The EDX spectrum of the attained $\{\text{Fe}_3\text{O}_4@\text{SiO}_2@(\text{CH}_2)_3\text{Semicarbazide-SO}_3\text{H/HCl}\}$ as MNP catalyst indicates the presence of the anticipated elements in the structure of the catalyst, for example carbon (C), nitrogen (N), iron (Fe), oxygen (O), silicon (Si), sulfur (S) and chlorine (Cl) (Fig. 3). It is clearly revealed that the synthesized MNP catalyst contains only C, N, Fe, O, Si, S and Cl elements. No extra peaks related to any impurity are identified with SEM coupled EDX, which means that the MNP catalyst is composed only of C (6.88), N (6.88), Fe (22.18), O (50.58), Si (46.30), S (16.52) and Cl (0.70), which is shown by the elemental analysis.

The TGA curve of the $\{\text{Fe}_3\text{O}_4@\text{SiO}_2@(\text{CH}_2)_3\text{Semicarbazide-SO}_3\text{H/HCl}\}$ as MNP catalyst displays a mass loss of organic material as it decomposes upon heating (Fig. 4). The primary weight loss from the MNP catalyst (room temperature to 120°C) is owing to the removal of physically adsorbed water and organic solvents, which were used in the course of the synthesis of the catalyst. The weight

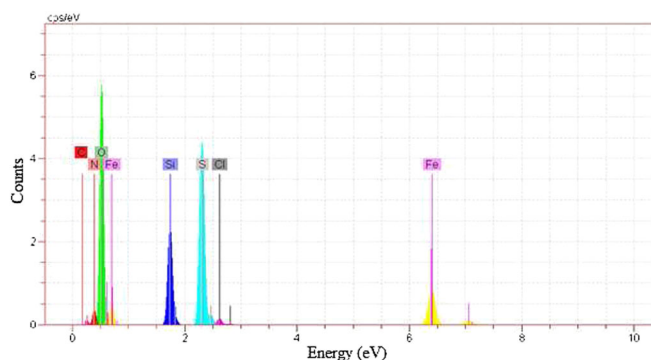


Figure 3. EDX spectrum of $\{\text{Fe}_3\text{O}_4@\text{SiO}_2@(\text{CH}_2)_3\text{Semicarbazide-SO}_3\text{H/HCl}\}$ as MNP catalyst.

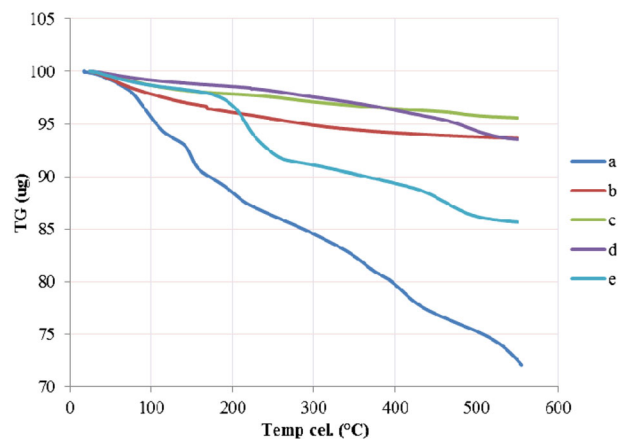


Figure 4. TGA curves: (a) $\{\text{Fe}_3\text{O}_4@\text{SiO}_2@(\text{CH}_2)_3\text{Semicarbazide-SO}_3\text{H/HCl}\}$; (b) Fe_3O_4 ; (c) $\text{Fe}_3\text{O}_4@\text{SiO}_2$; (d) $\text{Fe}_3\text{O}_4@\text{SiO}_2@(\text{CH}_2)_3\text{-Cl}$; (e) $\text{Fe}_3\text{O}_4@\text{SiO}_2@(\text{CH}_2)_3\text{Semicarbazide}$.

loss is about 7%. The weight loss (14%) between 120 and 410°C is attributed chiefly to the thermal decomposition of semicarbazide functionalized with chlorosulfonic acid on the surface of the silica coating. $\{\text{Fe}_3\text{O}_4@\text{SiO}_2@(\text{CH}_2)_3\text{Semicarbazide-SO}_3\text{H/HCl}\}$ displays three-step weight loss behaviour. A weight loss of MNP catalyst of about 5% appears at 410–510°C, which is attributed to the thermal decomposition of the MNP catalyst. As a result, the TGA of the MNP catalyst shows main loss in three steps, and decomposes after 510°C. The changes in TGA spectra confirm that material is added in each synthesis step.

The structures of Fe_3O_4 MNPs, $\text{Fe}_3\text{O}_4@\text{SiO}_2@(\text{CH}_2)_3\text{Semicarbazide}$ and $\{\text{Fe}_3\text{O}_4@\text{SiO}_2@(\text{CH}_2)_3\text{Semicarbazide-SO}_3\text{H/HCl}\}$ were investigated using XRD. The XRD pattern of the bare MNPs reveals a pattern consistent with those of spinel ferrites described (Fig. 5). The related peaks are identified in both of the $\{\text{Fe}_3\text{O}_4@\text{SiO}_2@(\text{CH}_2)_3\text{Semicarbazide-SO}_3\text{H/HCl}\}$ XRD patterns, indicating the retention of the crystalline spinel ferrite core structure during the reaction process. The positions and relative intensities of all peaks conform well with the standard XRD pattern of Fe_3O_4 MNPs (JCPDS card no. 85-1436) representing the retention of the crystalline cubic spinel structure of MNPs. The XRD patterns of the particles show nine characteristic peaks linked to a cubic iron oxide phase ($2\theta = 14.80^\circ, 30.10^\circ, 35.50^\circ, 43.10^\circ, 53.00^\circ, 57.00^\circ, 62.80^\circ, 70.50^\circ, 73.90^\circ$). These are revealed to their corresponding indices (1 1 0), (2 2 0), (3 1 1), (4 0 0), (3 3 1), (4 2 2), (5 1 1), (4 4 0) and (5 3 1), respectively. It is implicit that the resultant nanoparticles

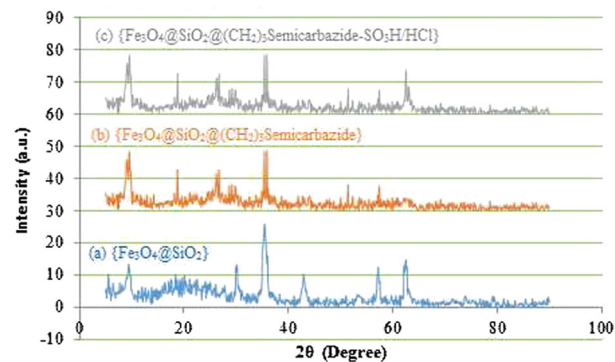


Figure 5. XRD patterns: (a) $\{\text{Fe}_3\text{O}_4@\text{SiO}_2\}$; (b) $\{\text{Fe}_3\text{O}_4@\text{SiO}_2@(\text{CH}_2)_3\text{Semicarbazide}\}$; (c) $\{\text{Fe}_3\text{O}_4@\text{SiO}_2@(\text{CH}_2)_3\text{Semicarbazide-SO}_3\text{H/HCl}\}$ as MNP catalyst.

are pure Fe_3O_4 with a spinel structure and that the grafting method does not induce any phase change of Fe_3O_4 . The size, shape and morphology of $\{\text{Fe}_3\text{O}_4@\text{SiO}_2@(\text{CH}_2)_3\text{Semicarbazide-SO}_3\text{H/HCl}\}$ as MNP catalyst were investigated using XRD, SEM, TEM and AFM analyses. The XRD pattern of the MNP catalyst was studied in the range 10–90° (Fig. 5). As revealed in Fig. 5, the XRD pattern shows diffraction lines of highly crystalline nature at $2\theta = 18.80^\circ, 26.20^\circ, 26.70^\circ, 28.70^\circ, 29.20^\circ, 29.80^\circ, 35.40^\circ, 35.90^\circ, 51.40^\circ, 57.40^\circ, 62.50^\circ$ and 63.00° . The peak width (FWHM), size and interplanar distance from the XRD pattern of $\{\text{Fe}_3\text{O}_4@\text{SiO}_2@(\text{CH}_2)_3\text{Semicarbazide-SO}_3\text{H/HCl}\}$ in the range 18.80–63.00° were obtained and the results are summarized in Table 1. For example, assignments for the highest diffraction line, 35.90°, reveal a FWHM of 0.13 and a crystalline size for the catalyst of ca 64.24 nm through the Debye–Scherrer equation: $D = K\lambda/(\beta\cos\theta)$ (where D is the crystalline size, K is the shape factor, corresponding to 0.9, λ is the X-ray wavelength, β is the FWHM of the diffraction peak and θ is the Bragg diffraction angle in degrees). An interplanar distance of 0.249848 nm (from the highest diffraction line at 35.90°) is found via the Bragg equation: $d_{hkl} = \lambda/(2\sin\theta)$, where λ is Cu radiation wavelength (0.154178 nm). Crystallite sizes obtained from numerous diffraction lines using the Debye–Scherrer equation are found to be in the nanometre range (18.97–64.24 nm), which is chiefly in good agreement with the results obtained from SEM and TEM (Fig. 6). In general, with addition of reactants in each stage, XRD patterns confirm the synthesis of the catalyst in each step. Changes in XRD patterns indicate that the materials are attached as a tag in each synthesis step (nevertheless the general structure of XRD patterns is kept).

AFM is a method that allows the determination and analysis of surfaces with high resolution. AFM has abundant advantages, and practically any typical surface can be imaged: for example hard surfaces such as the surface of a ceramic material, or the dispersal of a metallic nanocomposite; or very soft, for example molecules of proteins or plastic materials. Figure 7 displays the two- and three-dimensional AFM images of $\{\text{Fe}_3\text{O}_4@\text{SiO}_2@(\text{CH}_2)_3\text{Semicarbazide-SO}_3\text{H/HCl}\}$ as MNP catalyst. No important partition area in size is identified in the images. After studying the three-dimensional $2.1\ \mu\text{m}^2 \times 2.1\ \mu\text{m}^2$ frameworks, we can understand that the obtained MNP catalyst has an interrupted structure with a desirable external planarity. The surface of the coat on the MNP catalyst is visibly revealed to be less than 65 nm.

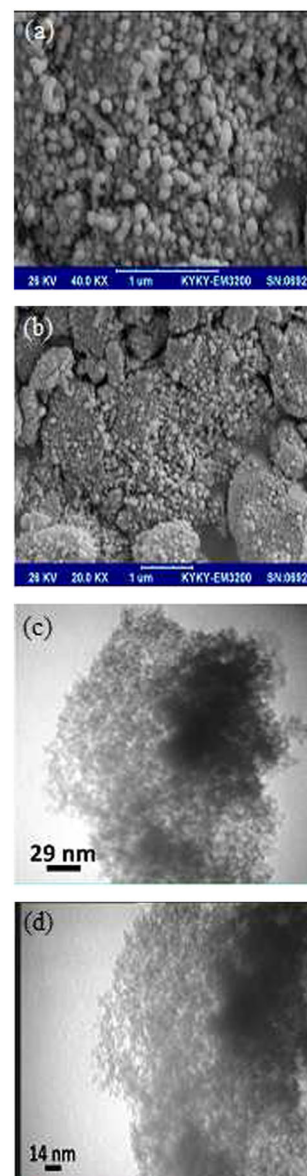


Figure 6. (a, b) SEM images and (c, d) TEM images of $\{\text{Fe}_3\text{O}_4@\text{SiO}_2@(\text{CH}_2)_3\text{Semicarbazide-SO}_3\text{H/HCl}\}$ as MNP catalyst.

Entry	2θ	Peak width (FWHM) (°)	Size (nm)	Interplaner distance (nm)
1	18.80	0.20	40.27	0.471450
2	26.20	0.43	18.97	0.339729
3	26.70	0.26	31.40	0.333479
4	28.70	0.17	48.23	0.310678
5	29.20	0.16	51.32	0.305472
6	29.80	0.41	20.05	0.299456
7	35.40	0.23	36.26	0.253262
8	35.90	0.13	64.24	0.249848
9	51.40	0.15	58.78	0.177559
10	57.40	0.18	50.32	0.160409
11	62.50	0.33	28.16	0.148427
12	63.00	0.38	24.52	0.147369

Magnetic measurements of the Fe_3O_4 nanoparticles and the MNP catalyst were conducted at room temperature using a vibrating sample magnetometer. Based on the magnetization curves (Fig. 8), the saturation magnetization of the obtained MNP catalyst decreases from $52\ \text{emu g}^{-1}$ (Fe_3O_4) to $11\ \text{emu g}^{-1}$. This reduction in saturation magnetization is due to the surface coating on the Fe_3O_4 nanoparticles.

Application of $\{\text{Fe}_3\text{O}_4@\text{SiO}_2@(\text{CH}_2)_3\text{Semicarbazide-SO}_3\text{H/HCl}\}$ as MNP catalyst in synthesis of 3,3'-(Arylmethylene)bis(4-hydroxycoumarin) derivatives

Initially, to optimize the reaction conditions, the condensation reaction of 4-chlorobenzaldehyde with 4-hydroxycoumarin was selected as a model and various amounts of $\{\text{Fe}_3\text{O}_4@\text{SiO}_2@(\text{CH}_2)_3\text{Semicarbazide-SO}_3\text{H/HCl}\}$ as MNP catalyst were used from room temperature to 100°C under solvent-free conditions (Table 2). As

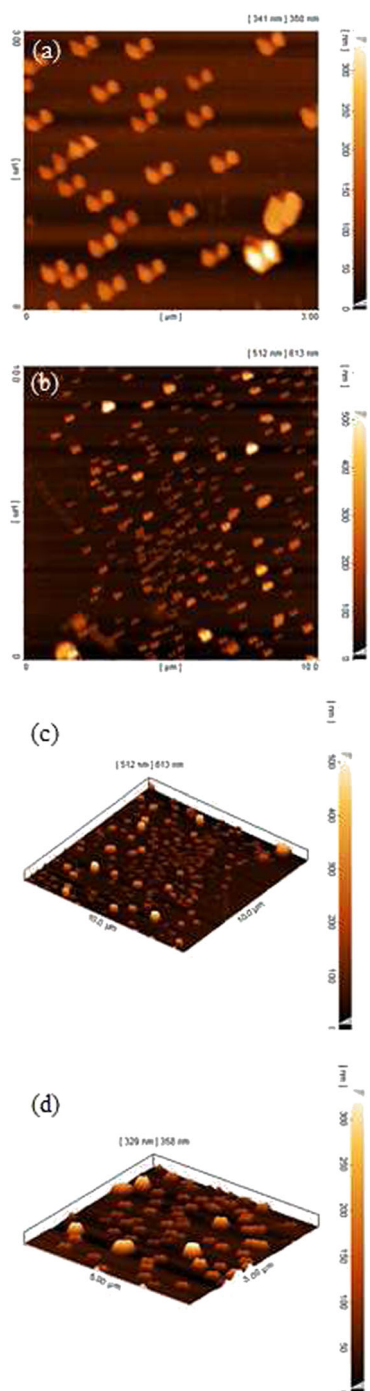


Figure 7. (a, b) Two-dimensional and (c, d) three-dimensional AFM images of $\text{Fe}_3\text{O}_4@SiO_2@(CH_2)_3\text{Semicarbazide-SO}_3\text{H/HCl}$ as MNP catalyst.

evident from Table 2, the best results are obtained when the reaction is conducted using 0.01 g of MNP catalyst at 80°C (Table 2, entry 9). No improvement is observed in the yield through increasing the amount of catalyst and temperature (Table 2, entries 10–13). In the absence of MNP catalyst, the product is not obtained (Table 2, entry 1).

Moreover, to compare the results of the reaction in solution with those of solvent-free conditions, a mixture of 4-chlorobenzaldehyde with 4-hydroxycoumarin as a typical reaction, using 10 mg of MNP catalyst in various solvents, i.e. water, CH_3CN , $\text{C}_2\text{H}_5\text{OH}$, $\text{CH}_3\text{CO}_2\text{Et}$ and toluene, was considered at 80°C (Table 3). As can

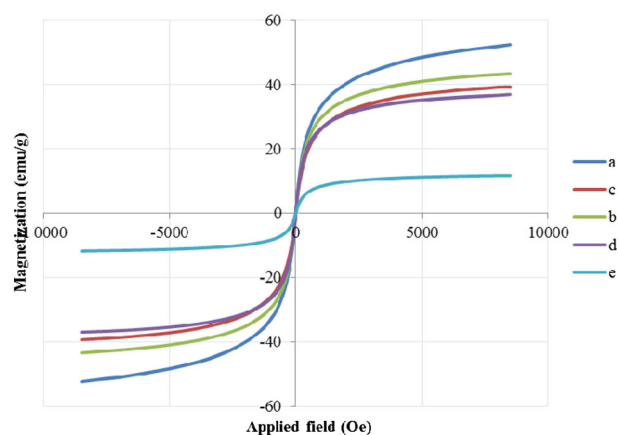


Figure 8. Vibrating sample magnetometry curves: (a) Fe_3O_4 ; (b) $\text{Fe}_3\text{O}_4@SiO_2$; (c) $\text{Fe}_3\text{O}_4@SiO_2@(CH_2)_3\text{-Cl}$; (d) $\text{Fe}_3\text{O}_4@SiO_2@(CH_2)_3\text{Semicarbazide}$; (e) $\text{Fe}_3\text{O}_4@SiO_2@(CH_2)_3\text{Semicarbazide-SO}_3\text{H/HCl}$.

Table 2. Result of amount of catalyst and temperature in synthesis of 3,3'-(arylmethylene)bis(4-hydroxycoumarin) derivatives under solvent-free conditions^a

Entry	Catalyst loading (mg)	Reaction temperature (°C)	Reaction time (min)	Yield (%) ^b
1	Catalyst-free	80	180	No reaction
2	1	80	90	40
3	3	80	90	55
4	5	80	90	86
5	7	80	70	90
6	10	r.t.	180	No reaction
7	10	40	180	60
8	10	60	90	75
9	10	80	20	98
10	10	90	20	98
11	10	100	20	98
12	15	80	30	97
13	20	80	27	98

^aReaction conditions: 4-chlorobenzaldehyde (1 mmol), 4-hydroxycoumarin (2 mmol).
^bIsolated yield.

Table 3. Effect of solvent in synthesis of 3,3'-(arylmethylene)bis(4-hydroxycoumarin) derivatives^a

Entry	Solvent	Reaction time (min)	Yield (%) ^b
1	CH_3CN	45	95
2	H_2O	60	37
3	$\text{C}_2\text{H}_5\text{OH}$	30	95
4	$\text{CH}_3\text{CO}_2\text{Et}$	60	83
5	Toluene	60	51
6	Solvent-free	20	98

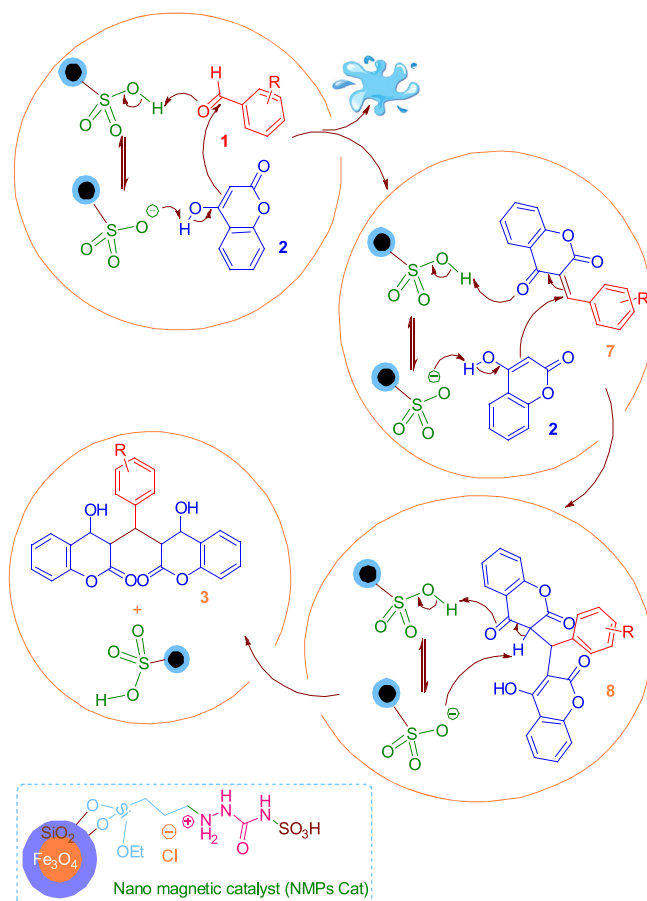
^aReaction conditions: 4-Chlorobenzaldehyde (1 mmol), 4-hydroxycoumarin (2 mmol).
^bIsolated yield.

be seen, solvent-free conditions give the best results for this reaction.

After identifying the optimum reaction conditions, the reaction was performed with aromatic aldehydes and 4-hydroxycoumarin.

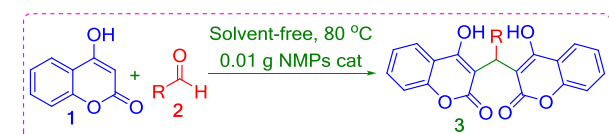
To show the generality of the described procedure, numerous aldehydes were reacted with two equivalents of 4-hydroxycoumarin under the same conditions. These results encouraged us to study the scope, limitations and overview of this process for various aldehydes under optimized conditions. As evident from Table 4, a series of aromatic aldehydes undergo electrophilic substitution reaction with 4-hydroxycoumarin to provide a series of substituted 3,3'-(arylmethylene)bis(4-hydroxycoumarin) derivatives in high to excellent yields. The nature and electronic properties of the substituents on the aromatic ring affect the conversion rate, with aromatic aldehydes possessing electron-withdrawing groups (Table 4, entries 3 and 4) on the aromatic ring reacting faster than those with electron-donating groups (Table 4, entries 10, 12 and 14).

A suggested simple and satisfactory mechanism for the synthesis of 3,3'-(arylmethylene)bis(4-hydroxycoumarin) derivatives catalysed by $\{\text{Fe}_3\text{O}_4@\text{SiO}_2@(\text{CH}_2)_3\text{Semicarbazide-SO}_3\text{H}/\text{HCl}\}$ is shown in Scheme 2. According to the reaction procedure, initially the MNP catalyst activates the carbonyl group of the aromatic aldehyde (by H^+ from SO_3H moiety-catalysed) and then completed Knoevenagel condensation of nucleophilic attack of activated 4-hydroxycoumarin (by SO_3^- moiety-catalysed) and via elimination of one molecule of H_2O forms intermediate **7**. In the next step, the MNP catalyst activates the carbonyl group of intermediate **7** (by H^+ from SO_3H moiety-catalysed) and nucleophilic attack of a second equivalent of activated 4-hydroxycoumarin (by SO_3^- moiety-catalysed) through Michael addition creates α,β -unsaturated ketone (intermediate **8**). Finally, this catalytic cycle is completed by removal of H^+ in an enolization process and thus the product is prepared in the presence of the MNP catalyst.^[59]



Scheme 2. Probable mechanism for the synthesis of 3,3'-(arylmethylene)bis(4-hydroxycoumarin) derivatives catalysed by $\{\text{Fe}_3\text{O}_4@\text{SiO}_2@(\text{CH}_2)_3\text{Semicarbazide-SO}_3\text{H}/\text{HCl}\}$ MNPs.

Table 4. Synthesis of 3,3'-(arylmethylene)bis(4-hydroxycoumarin) derivatives using 0.01 g of $\{\text{Fe}_3\text{O}_4@\text{SiO}_2@(\text{CH}_2)_3\text{Semicarbazide-SO}_3\text{H}/\text{HCl}\}$ as MNP catalyst^a



Entry	Aldehyde	Time (min)	Yield (%) ^b	M.p. (Lit.) (°C)
1	Benzaldehyde	30	95	233–235 (229–231) ^[59]
2	3-Nitrobenzaldehyde	15	92	225–227 (214–215) ^[59]
3	4-Nitrobenzaldehyde	10	97	230–231 (233–235) ^[59]
4	4-Chlorobenzaldehyde	20	98	240–242 (261–263) ^[59]
5	3-Chlorobenzaldehyde	30	93	234–236 (221–223) ^[59]
6	2-Chlorobenzaldehyde	20	95	208–210 (201–203) ^[59]
7	3-Fluorobenzaldehyde	20	96	217–218 (white solid)
8	Pyridine-4-carbaldehyde	40	91	267–269
9	3-Ethoxy-4-hydroxybenzaldehyde	40	95	218–219 (cream solid)
10	3-Methoxybenzaldehyde	40	93	249–250 (250–252) ^[59]
11	Terephthalaldehyde	90	89	296–297 ^[12]
12	3-Hydroxybenzaldehyde	50	92	227–229 (210.5) ^[59]
13	4-Hydroxybenzaldehyde	50	95	219–221 (193) ^[59]
14	4-Cyanobenzaldehyde	20	96	235–237 (260–262) ^[59]
15	4-Methylbenzaldehyde	35	96	270–271 (266–269) ^[59]

^aReaction conditions: aldehyde (1 mmol), 4-hydroxycoumarin (2 mmol).

^bIsolated yield.

In addition, considering the magnetic separation and isolation of the MNP catalyst on reaction completion (reaction between 4-chlorobenzaldehyde and 4-hydroxycoumarin), recyclability and reusability of the MNP catalyst for numerous runs were also studied. Results shown in Fig. 9 confirm that the magnetically separable MNP catalyst could be reused and recycled eight times without

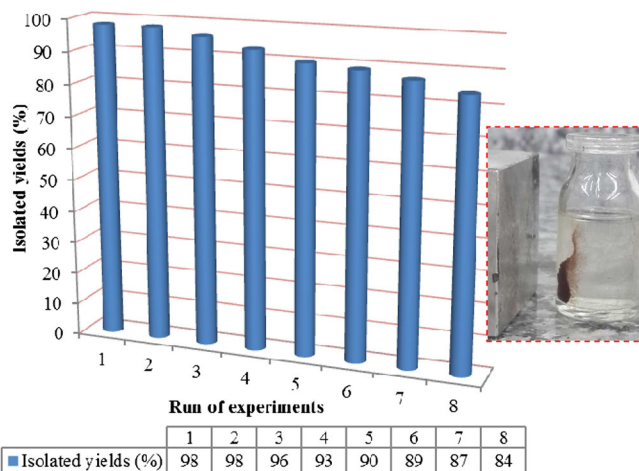


Figure 9. Reusability of the $\{\text{Fe}_3\text{O}_4@\text{SiO}_2@(\text{CH}_2)_3\text{Semicarbazide-SO}_3\text{H}/\text{HCl}\}$ MNP catalyst for the synthesis of 3,3'-(arylmethylene)bis(4-hydroxycoumarin) in 20 min.

any noteworthy loss of its initial catalytic activity. The reaction was scaled up to 10 mmol of 4-chlorobenzaldehyde and 4-hydroxycoumarin in the presence of 0.1 g of MNP catalyst at 80°C. The yield of the reaction is 98% in 20 min and 84% after the eighth run. The results are summarized in Fig. 9.

Application of $\{Fe_3O_4@SiO_2@(CH_2)_3\text{Semicarbazide-SO}_3H/HCl\}$ as MNP catalyst in synthesis of 1-Carbamato-alkyl-2-naphthol derivatives

To optimize the reaction conditions, the condensation reaction of 4-chlorobenzaldehyde with benzyl carbamate and β -naphthol was chosen as a model and various amounts of MNP catalyst at room temperature to 100°C were tested under solvent-free conditions (Table 5). As evident from Table 5, the best results are achieved when the reaction is conducted in the presence of 7 mg of MNP catalyst at 70°C (Table 5, entry 8). No improvement is identified in the yield of the reaction through increasing the amount of the MNP catalyst and the temperature (Table 5, entries 9 and 13). It is clear that in the absence of the MNP catalyst, the product is not obtained (Table 5, entry 1).

To compare the results for solution with those for solvent-free conditions, a mixture of 4-chlorobenzaldehyde, benzyl carbamate and β -naphthol as a typical reaction in the presence of 7 mg of MNP catalyst in various solvents, i.e. water, C_2H_5OH , CH_3CN , CH_3CO_2Et and toluene, was studied at 70°C (Table 6). Solvent-free conditions give the best results for this reaction.

Following optimization of the reaction conditions, to probe the efficacy and the scope of the process, various 1-carbamato-alkyl-2-naphthol derivatives were synthesized via the one-pot three-component condensation reaction between aromatic aldehydes with benzyl carbamate and β -naphthol in the presence of catalytic amounts of $\{Fe_3O_4@SiO_2@(CH_2)_3\text{Semicarbazide-SO}_3H/HCl\}$ under solvent-free reaction conditions. The results are summarized in Table 7. The effect of substituents on the aromatic ring is seen to be strong in terms of yields under these reaction conditions. Both types of aromatic aldehydes with electron-releasing and electron-withdrawing substituents on their aromatic ring give suitable products in high to excellent yields in short reaction times. The reaction

Table 5. Result of amount of catalyst and temperature in synthesis of 1-carbamato-alkyl-2-naphthol derivatives under solvent-free conditions^a

Entry	Catalyst loading (mg)	Reaction temperature (°C)	Reaction time (min)	Yield (%) ^b
1	Catalyst-free	80	180	No reaction
2	1	80	180	50
3	3	80	60	85
4	5	80	30	95
5	7	r.t.	180	No reaction
6	7	40	180	40
7	7	60	30	93
8	7	70	10	98
9	7	80	10	98
10	7	90	10	98
11	7	100	10	96
12	10	70	10	98
13	15	70	8	96

^aReaction conditions: 4-chlorobenzaldehyde (1 mmol), β -naphthol (1 mmol), benzyl carbamate (1.1 mmol).

^bIsolated yield.

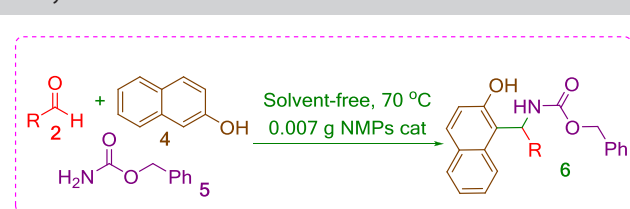
Table 6. Effect of solvent in synthesis of 1-carbamato-alkyl-2-naphthol derivatives^a

Entry	Solvent	Reaction time (min)	Yield (%) ^b
1	H ₂ O	180	7
2	C ₂ H ₅ OH	60	21
3	CH ₃ CN	60	15
4	CH ₃ CO ₂ Et	120	15
5	Toluene	120	11
6	Solvent-free	10	98

^aReaction conditions: 4-chlorobenzaldehyde (1 mmol), β -naphthol (1 mmol), benzyl carbamate (1.1 mmol).

^bIsolated yield.

Table 7. Synthesis of 1-carbamato-alkyl-2-naphthol derivatives using 0.01 g of $\{Fe_3O_4@SiO_2@(CH_2)_3\text{Semicarbazide-SO}_3H/HCl\}$ as MNP catalyst^{a,b}

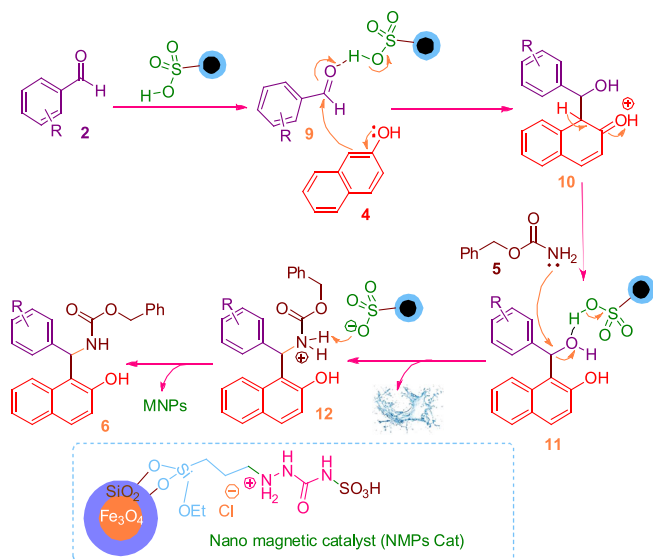


Entry	Aldehyde	Time (min)	Yield (%) ^b	M.p. (Lit.) (°C)
1	Pyridine-4-carbaldehyde	20	88	205–206 (cream solid)
2	Benzaldehyde	15	96	186–188 (179–180) ^[60]
3	2-Nitrobenzaldehyde	10	90	204–205 (198–200) ^[60]
4	3-Nitrobenzaldehyde	12	92	197–198 (196–197) ^[60]
5	4-Nitrobenzaldehyde	8	96	200–202 (200) ^[60]
6	4-Chlorobenzaldehyde	10	98	178–179 (176–177) ^[60]
7	3-Chlorobenzaldehyde	10	94	185–186 (183–185) ^[60]
8	2-Chlorobenzaldehyde	10	97	207–209 (214–216) ^[60]
9	2,3-Dichlorobenzaldehyde	10	95	209–210
10	2,4-Dichlorobenzaldehyde	5	97	207–209 (202–204) ^[60]
11	4-Chloro-3-nitrobenzaldehyde	5	97	212–214 (pale yellow solid)
12	4-Fluorobenzaldehyde	5	96	197–198 (202–203) ^[60]
13	3-Fluorobenzaldehyde	10	91	197–199 (185–186) ^[60]
14	4-Bromobenzaldehyde	5	93	177–178 (180–182) ^[60]
15	4-Methylbenzaldehyde	30	90	151–153 (152–154) ^[60]
16	2-Methoxybenzaldehyde	30	92	196–198 (202–204) ^[60]
17	Naphtalene-1-carbaldehyde	20	91	207–208
18	Naphtalene-2-carbaldehyde	20	93	194–195

^aReaction conditions: aldehyde (1 mmol), β -naphthol (1 mmol), benzyl carbamate (1.1 mmol).

^bIsolated yield.

of aromatic aldehydes possessing electron-withdrawing groups (Table 7, entries 5 and 6) is faster than that of aldehydes with electron-donating groups (Table 7, entries 15 and 16). Additionally, recyclability and reusability of the catalyst were also studied for the condensation of 4-chlorobenzaldehyde with benzyl carbamate and β -naphthol. Correspondingly, the MNP catalyst was separated and reused for further reaction.



Scheme 3. Plausible mechanism for the synthesis of 1-carbamato-alkyl-2-naphthol derivatives catalysed by $\{\text{Fe}_3\text{O}_4@ \text{SiO}_2@ (\text{CH}_2)_3 \text{Semicarbazide-SO}_3\text{H/Cl}\}$ MNPs.

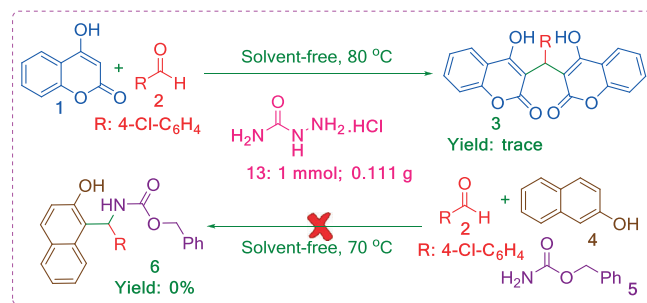
In Scheme 3, we propose a probable mechanism for the synthesis of 1-carbamato-alkyl-2-naphthol derivatives in the presence of $\{\text{Fe}_3\text{O}_4@ \text{SiO}_2@ (\text{CH}_2)_3 \text{Semicarbazide-SO}_3\text{H/Cl}\}$ as MNP catalyst. As regards the reaction process, firstly the MNP catalyst activates the carbonyl group of the aromatic aldehyde (by H^+ from SO_3H moiety-catalysed) and then nucleophilic attack of activated β -naphthol (by SO_3^- moiety-catalysed) and via elimination of one molecule of H_2O forms *ortho*-quinone methide intermediate **11**. A practical description for this result can be given by studying the nucleophilic addition of benzyl carbamate to intermediate **11**. Finally the anticipated product is obtained after aromatization.^[47,48,60]

To compare the efficiency of our catalyst with that of catalysts reported by others for the synthesis of 3,3'-(arylmethylene)bis(4-hydroxycoumarin) derivatives, Table 8 summarizes the results for catalysts in the condensation of 4-chlorobenzaldehyde with 4-hydroxycoumarin. As is evident, the MNP catalyst improves the synthesis of product.

According to the suggested reaction mechanism, the presence of hydrochloride salt moiety does not affect the progress of reactions. To illustrate this issue, the reactions between 4-hydroxycoumarin and 4-chlorobenzaldehyde (in the synthesis of 3,3'-(arylmethylene)bis(4-hydroxycoumarin)) and

Table 8. Comparison of results for synthesis of model product by MNP catalyst with those obtained using other reported catalysts

Entry	Reaction conditions	Catalyst amount	Time (min)	Yield (%)	Ref.
1	MNP catalyst, 80°C	10 mg	20	80	This work
2	TBAB, H_2O , 100°C	10 mol%	30	95	[26]
3	TBAB, solvent-free, 100°C	10 mol%	20	87	[26]
4	[MIM $(\text{CH}_2)_4\text{SO}_3\text{H}$], solvent-free, 80°C	15 mol%	25	93	[59]
5	SBPPSP, $\text{H}_2\text{O}/\text{C}_2\text{H}_5\text{OH}$, reflux	60 mg	15	95	[59]
6	$\text{RuCl}_3 \cdot n\text{H}_2\text{O}$, H_2O , 80°C	5 mol%	25	85	[61]
7	Nano SiO_2Cl , CH_2Cl_2 , 40°C	75 mg	180	92	[62]
8	SDS, H_2O , 60°C	20 mol%	150	93	[63]



Scheme 4. Synthesis of 3,3'-(arylmethylene)bis(4-hydroxycoumarin) and 1-carbamato-alkyl-2-naphthol in the presence of semicarbazide hydrochloride.

4-chlorobenzaldehyde, benzyl carbamate and β -naphthol (in the synthesis of 1-carbamato-alkyl-2-naphthol) were investigated under the same reaction conditions in the presence of 1 mmol of semicarbazide hydrochloride. The 3,3'-(arylmethylene)bis(4-hydroxycoumarin) is synthesized in trace yield and the 1-carbamato-alkyl-2-naphthol is not produced (Scheme 4).

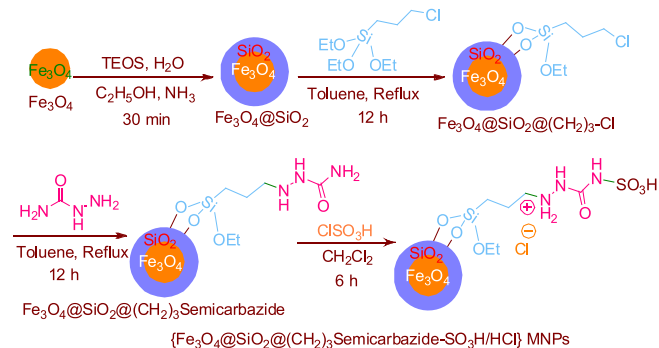
Conclusions

In summary, a novel, reusable, green and mild semicarbazide-based ionic liquid stabilized on silica-coated Fe_3O_4 MNPs, namely $\{\text{Fe}_3\text{O}_4@ \text{SiO}_2@ (\text{CH}_2)_3 \text{Semicarbazide-SO}_3\text{H/Cl}\}$, was designed, synthesized and fully characterized using FT-IR, UV-visible and EDX spectroscopies, TGA, XRD, SEM, TEM and AFM. Application of this catalyst was studied for the synthesis of 3,3'-(arylmethylene)bis(4-hydroxycoumarin) derivatives and one-pot three-component condensation reaction of aromatic aldehydes with benzyl carbamate and β -naphthol at 70°C (synthesis of 1-carbamato-alkyl-2-naphthol derivatives) under efficient, green, mild and solvent-free conditions. Significant advantages of the catalyst are relative environmental benignity, cleaner reaction profile, simplicity of product isolation, short reaction time, high yield, recyclability and reusability, in close agreement with the green chemistry disciplines. To the best of our knowledge, this is the first report of the synthesis of semicarbazide-based ionic liquid stabilized on silica-coated Fe_3O_4 MNPs. Consequently the current study can open up a novel and promising insight into the sequence of rational design, synthesis and applications of task-specific nanomagnetic ionic liquids with desirable properties as full-fledged substances for maintainable acid-catalysed chemical processes.

Experimental

General procedure for preparation of $\{\text{Fe}_3\text{O}_4@ \text{SiO}_2@ (\text{CH}_2)_3 \text{Semicarbazide-SO}_3\text{H/Cl}\}$ catalyst

Firstly, magnetite phase Fe_3O_4 was prepared by adding 3 ml of FeCl_3 (2 M dissolved in 2 M HCl) to 10.33 ml of double-distilled water followed by dropwise addition of 2 ml of Na_2SO_3 (1 M) for 3 min under magnetic stirring. With a change of colour from red to light yellow in the solution, 80 ml of an $\text{NH}_3 \cdot \text{H}_2\text{O}$ solution (0.85 M) was added under vigorous stirring. Subsequently after 15 min, the



Scheme 5. Synthesis of $\{\text{Fe}_3\text{O}_4@\text{SiO}_2@(\text{CH}_2)_3\text{Semicarbazide-SO}_3\text{H/HCl}\}$ MNPs.

magnetite precipitate (Fe_3O_4) was washed to $\text{pH} < 7.5$ with distilled water and separated with a magnet.^[64]

A mixture containing 1 g of Fe_3O_4 , 20 ml of water, 80 ml of ethanol, 3 ml of ammonia and 3 ml of tetraethylorthosilicate (TEOS) was refluxed to afford silica-coated Fe_3O_4 ($\text{Fe}_3\text{O}_4@\text{SiO}_2$).^[65] Subsequently, 3 g of $\text{Fe}_3\text{O}_4@\text{SiO}_2$ and (3-chloropropyl)triethoxysilane (10 mmol) in 80 ml of dry toluene were refluxed under nitrogen for 12 h. The obtained $\text{Fe}_3\text{O}_4@\text{SiO}_2@(\text{CH}_2)_3\text{-Cl}$ (grafted with chloropropyl group) was filtered, washed twice with dry toluene and anhydrous diethyl ether, and dried at 80°C for 6 h in vacuum. Then semicarbazide (0.751 g, 10 mmol) in 50 ml of dry toluene was added to the $\text{Fe}_3\text{O}_4@\text{SiO}_2@(\text{CH}_2)_3\text{Cl}$ and the mixture was refluxed for 12 h. The resulting solid was filtered, washed and dried in a similar process to afford $\text{Fe}_3\text{O}_4@\text{SiO}_2@(\text{CH}_2)_3\text{-Semicarbazide}$.

Finally, chlorosulfonic acid (1.165 g, 10 mmol) was added dropwise to the $\text{Fe}_3\text{O}_4@\text{SiO}_2@(\text{CH}_2)_3\text{-Semicarbazide}$ in dry dichloromethane and the mixture was stirred for 6 h. Then with similar steps of filtering, washing and drying, $\{\text{Fe}_3\text{O}_4@\text{SiO}_2@(\text{CH}_2)_3\text{Semicarbazide-SO}_3\text{H/HCl}\}$ as MNP catalyst was obtained. The synthetic route to the described catalyst is shown in Scheme 5.

General procedure for synthesis of 3,3'-(Arylmethylene)bis(4-hydroxycoumarin) derivatives

To a mixture of aromatic aldehyde (1 mmol) and 4-hydroxycoumarin (0.324 g, 2 mmol) was added 10 mg of $\{\text{Fe}_3\text{O}_4@\text{SiO}_2@(\text{CH}_2)_3\text{Semicarbazide-SO}_3\text{H/HCl}\}$ MNPs followed by mixing under solvent-free conditions at 80°C for the appropriate time given in Table 3. After completion of the reaction, which was determined with TLC (*n*-hexane–ethyl acetate, 5:2), the MNP catalyst was recovered magnetically and the mixture was purified via recrystallization from ethanol–water (10:1), which resulted in precipitation of the anticipated 3,3'-(arylmethylene)bis(4-hydroxycoumarin) derivatives. All of the products were identified by comparison of their physical data with those of known compounds (supporting information).

General procedure for synthesis of 1-Carbamato-alkyl-2-naphthol derivatives

To a mixture of aromatic aldehyde (1 mmol), benzyl carbamate (0.151 g, 1 mmol) and β -naphthol (0.144 g, 1 mmol) was added 7 mg of $\{\text{Fe}_3\text{O}_4@\text{SiO}_2@(\text{CH}_2)_3\text{Semicarbazide-SO}_3\text{H/HCl}\}$ MNPs followed by mixing under solvent-free conditions at 70°C for the appropriate time given in Table 5. After completion of the reaction, which was determined with TLC (*n*-hexane–ethyl acetate, 5:2), the MNP catalyst was recovered magnetically and the mixture was purified

by recrystallization from ethanol–water (10:1), which resulted in precipitation of the desired 1-carbamato-alkyl-2-naphthol derivatives. All of the products were identified by comparison of their physical data with those of known compounds (supporting information).

Acknowledgments

We thank Bu-Ali Sina University and Iran National Science Foundation (INSF) for financial support of our research group.

References

- [1] M. A. Zolfigol, R. Ayazi, S. Bagheri, *RSC Adv.* **2015**, *5*, 71942.
- [2] a) M. Kaur, S. Sharma, P. M. S. Bedi, *Chin. J. Catal.* **2015**, *36*, 520. See reviews: b) P. Gupta, S. Paul, *Catal. Today.* **2014**, *236*, 153. c) M. M. Heravi, Z. Faghihi, *J. Iran. Chem. Soc.* **2014**, *11*, 209.
- [3] a) K. Tanabe, T. Yamagushi, T. T. Akeshita, *J. Res. Inst. Hokkaido Univ.* **1968**, *16*, 425. b) Y. C. Sharma, B. Singh, *Biofuels. Bioprod. Biorefin.* **2011**, *5*, 69.
- [4] a) S. Rostamnia, E. Doustkhaha, *Synlett* **2015**, *26*, 1345. b) K. Zeng, Z. Huang, J. Yang, Y. Gu, *Chin. J. Catal.* **2015**, *36*, 1606. c) X. Pan, M. Li, Y. Gu, *Chem. Asian J.* **2014**, *9*, 268. d) M. Li, A. Taheri, M. Liu, S. Sun, Y. Gu, *Adv. Synth. Catal.* **2014**, *356*, 537.
- [5] a) B. Karimi, F. Mansouri, H. M. Mirzaei, *Chem. Cat. Chem.* **2015**, *7*, 1736. See reviews: b) T. Cheng, D. Zhang, H. Li, G. Liu, *Green Chem.* **2014**, *16*, 3401. c) M. B. Gawande, R. Luque, R. Zboril, *Chem. Cat. Chem.* **2014**, *6*, 3312. d) D. Zhang, C. Zhou, Z. Sun, L. Wu, C. Tunga, T. Zhang, *Nanoscale* **2012**, *4*, 6244.
- [6] a) A. Schatz, O. Reiser, W. J. Stark, *Chem. Eur. J.* **2010**, *16*, 8950. b) D. Astruc, F. Lu, J. R. Aranzas, *Angew. Chem. Int. Ed.* **2005**, *44*, 7852.
- [7] A. H. Lu, E. L. Salabas, F. Schith, *Angew. Chem. Int. Ed.* **2007**, *46*, 1222.
- [8] S. Laurent, D. Forge, M. Port, A. Roch, C. Robic, L. V. Elst, R. N. Muller, *Chem. Rev.* **2008**, *108*, 2064.
- [9] S. C. Basa, *Phytochemistry* **1988**, *27*, 1933.
- [10] R. D. H. Murray, J. Medez, S. A. Brown, *The Natural Coumarins: Occurrence, Chemistry and Biochemistry*, Wiley, New York, **1982**.
- [11] M. I. Choudhary, N. Fatima, K. M. Khan, S. Jailil, S. Iqbal, Atta-ur-Rahman. *Biorg. Med. Chem.* **2006**, *14*, 8066.
- [12] C. X. Su, J. F. Mouscadet, C. C. Chiang, H. J. Tsai, L. Y. Hsu, *Chem. Pharm. Bull.* **2006**, *54*, 682.
- [13] S. S. Li, Z. Gao, X. Feng, S. M. Hecht, *J. Nat. Prod.* **2004**, *67*, 1608.
- [14] B. Y. Park, B. S. Min, S. R. Oh, J. H. Kim, K. H. Bae, H. K. Lee, *Phytother. Res.* **2006**, *20*, 610.
- [15] F. Borges, F. Roleira, N. Milhazes, L. Santana, E. Uriarte, *Curr. Med. Chem.* **2005**, *12*, 887.
- [16] M. Mercop, I. Malvar, B. Hrvacic, S. Markovic, A. Filipovic-Sucic, B. Bosnjak, A. Cempuh-Klonkay, R. Rupcic, A. Hutinec, I. J. Elenkov, M. Mesic, Patent WO 2006111858, **2006**.
- [17] I. Manolov, C. Maichle-Moessmer, I. Nicolova, N. Danchev, *Arch. Pharm.* **2006**, *339*, 319.
- [18] R. Nagashima, G. Levy, R. A. O'Reilly, *J. Pharm. Sci.* **1968**, *57*, 1888.
- [19] A. Romeo, M. Prosdoci, Patent WO 9222545, **1992**.
- [20] E. Altieri, M. Cordaro, G. Grassi, F. Risitano, A. Scala, *Tetrahedron* **2010**, *66*, 9493.
- [21] M. V. R. Reddy, R. E. Premkumar, Patent WO 2006132947, **2006**.
- [22] I. Kostova, G. Momekov, *Eur. J. Med. Chem.* **2006**, *41*, 717.
- [23] I. Kostova, G. Momekov, M. Zaharieva, M. Karaivanova, *Eur. J. Med. Chem.* **2005**, *40*, 542.
- [24] J. Wang, D. Q. Shi, Q. Y. Zhuang, X. S. Wang, S. J. Tu, *Chin. J. Org. Chem.* **2005**, *25*, 926.
- [25] M. Kidwi, V. Bansal, P. Mothra, S. Saxena, R. K. Somvanshi, S. Dey, *J. Mol. Catal. A* **2007**, *268*, 76.
- [26] J. M. Khurana, S. Kumar, *Tetrahedron Lett.* **2009**, *50*, 4125.
- [27] S. Qadir, A. Dar, K. Zaman, *Synth. Commun.* **2008**, *38*, 3490.
- [28] G. X. Gong, J. F. Zhou, L. T. An, X. L. Duan, S. J. Ji, *Synth. Commun.* **2009**, *39*, 497.
- [29] N. Hamdi, M. C. Puerta, P. Valerga, *Eur. J. Med. Chem.* **2008**, *43*, 2541.
- [30] T. Dingermann, D. Steinhilber, G. Folkers, *Molecular Biology in Medicinal Chemistry*, Wiley-VCH, Weinheim, **2004**.
- [31] A. Y. Shen, C. T. Tsai, C. L. Chen, *Eur. J. Med. Chem.* **1999**, *34*, 877.
- [32] A. Y. Shen, C. L. Chen, C. I. Lin, *Chin. J. Physiol.* **1992**, *35*, 45.

- [33] M. Damodiran, N. P. Selvam, P. T. Perumal, *Tetrahedron Lett.* **2009**, 50, 5474.
- [34] R. D. Clark, J. M. Caroon, A. F. Kluge, D. B. Repke, A. P. Roszkowski, A. M. Strosberg, S. Baker, S. M. Bitter, M. D. Okada, *J. Med. Chem.* **1983**, 26, 657.
- [35] H. Ren, S. Grady, D. Gamenara, H. Heinzen, P. Moyna, S. Croft, H. Kendrick, V. Yardley, G. Moyna, *Bioorg. Med. Chem. Lett.* **2001**, 11, 1851.
- [36] S. Remillard, L. I. Rebhun, G. A. Howie, S. M. Kupchan, *Science* **1975**, 189, 1002.
- [37] H. S. Mosher, M. B. Frankel, M. Gregory, *J. Am. Chem. Soc.* **1953**, 75, 5326.
- [38] F. Benedini, G. Bertolini, R. Cereda, G. Donà, G. Gromo, S. Levi, J. Mizrahi, A. Sala, *J. Med. Chem.* **1995**, 38, 130.
- [39] J. L. Peglion, J. Vian, B. Gourment, N. Despau, V. Audinot, M. Millan, *Bioorg. Med. Chem. Lett.* **1997**, 7, 881.
- [40] G. Y. Leshner, A. R. Surrey, *J. Am. Chem. Soc.* **1955**, 77, 636.
- [41] Y. Kusakabe, J. Nagatsu, M. Shibuya, O. Kawaguchi, C. Hirose, S. Shirato, *J. Antibiot.* **1972**, 25, 44.
- [42] H. Matsuoka, N. Ohi, M. Mihara, H. Suzuki, K. Miyamoto, N. Maruyama, K. Tsuji, N. Kato, T. Akimoto, Y. Takeda, K. Yano, T. Kuroki, *J. Med. Chem.* **1997**, 40, 105.
- [43] M. A. Zolfigol, A. Khazaei, A. R. Moosavi-Zare, A. Zare, V. Khakyzadeh, *Appl. Catal. A* **2011**, 400, 70.
- [44] A. Zare, S. Akbarzadeh, E. Foroozani, H. Kaveh, A. R. Moosavi-Zare, A. Hasaninejad, M. Mokhlesi, M. H. Beyzavi, M. A. Zolfigol, *J. Sulfur Chem.* **2012**, 33, 259.
- [45] V. K. Das, M. Borah, A. J. Thakur, *J. Org. Chem.* **2013**, 78, 3361.
- [46] A. Zare, H. Kaveh, M. Merajoddin, A. R. Moosavi-Zare, A. Hasaninejad, M. A. Zolfigol, *Phosph. Sulfur Silicon Relat. Elem.* **2013**, 188, 573.
- [47] H. Alinezhad, M. Tajbakhsh, M. Norouzi, S. Baghery, M. Akbari, *C. R. Chim.* **2014**, 17, 7.
- [48] M. A. Zolfigol, S. Baghery, A. R. Moosavi-Zare, S. M. Vahdat, H. Alinezhad, M. Norouzi, *RSC Adv.* **2015**, 5, 45027.
- [49] S. B. Patil, P. R. Singh, M. P. Surpur, S. D. Samant, *Synth. Commun.* **2007**, 37, 1659.
- [50] S. B. Patil, P. R. Singh, M. P. Surpur, S. D. Samant, *Ultrason. Sonochem.* **2007**, 14, 515.
- [51] H. R. Shaterian, H. Yarahmadi, M. Ghashang, *Tetrahedron* **2008**, 64, 1263.
- [52] A. Dorehgirae, H. Khabazzade, K. Saidi, *Arkivoc* **2009**, 7, 303.
- [53] a) D. Azarifar, S. M. Khatami, M. A. Zolfigol, R. Nejat-Yami, *J. Iran. Chem. Soc.* **2014**, 11, 1223. b) M. Safaiee, M. A. Zolfigol, M. Tavasoli, M. Mokhlesi, *J. Iran. Chem. Soc.* **2014**, 11, 1593.
- [54] M. A. Zolfigol, F. Shirini, P. Salehi, M. Abedini, *Curr. Org. Chem.* **2008**, 12, 183.
- [55] a) M. A. Zolfigol, T. Azadbakht, V. Khakizadeh, R. Nejatyami, D. Perrin, *RSC Adv.* **2014**, 4, 40036. b) T. Azadbakht, M. A. Zolfigol, R. Azadbakht, V. Khakizadeh, D. Perrin, *New J. Chem.* **2015**, 39, 439.
- [56] a) M. A. Zolfigol, S. Baghery, A. R. Moosavi-Zare, S. M. Vahdat, *RSC Adv.* **2015**, 5, 32933. b) A. R. Moosavi-Zare, M. A. Zolfigol, V. Khakyzadeh, C. Bottcher, M. H. Beyzavi, A. Zare, A. Hasaninejad, R. Luque, *J. Mater. Chem. A* **2014**, 2, 770. c) A. R. Moosavi-Zare, M. A. Zolfigol, O. Khaledian, V. Khakyzadeh, M. Darestani-Farahani, H. G. Kruger, *New J. Chem.* **2014**, 38, 2342. d) A. Khazaei, M. A. Zolfigol, A. R. Moosavi-Zare, Z. Asgari, M. Shekouhy, A. Zare, A. Hasaninejad, *RSC Adv.* **2012**, 2, 8010.
- [57] a) A. Taheri, X. Pan, C. Liu, Y. Gu, *Chem. Sus. Chem.* **2014**, 7, 2094. b) A. Taheri, B. Lai, C. Cheng, Y. Gu, *Green Chem.* **2015**, 17, 812. c) A. Taheri, C. Liu, B. Lai, C. Cheng, X. Pan, Y. Gu, *Green Chem.* **2014**, 16, 3715.
- [58] a) A. R. Moosavi-Zare, M. A. Zolfigol, M. Zarei, A. Zare, J. Afsar, *Appl. Catal. A* **2015**, 505, 224. b) A. R. Moosavi-Zare, M. A. Zolfigol, M. Zarei, A. Zare, V. Khakyzadeh, *J. Mol. Liq.* **2015**, 211, 373.
- [59] a) N. Tavakoli-Hoseini, M. M. Heravi, F. F. Bamoharram, A. Davoodnia, M. Ghassemzadeh, *J. Mol. Liq.* **2011**, 163, 122. b) K. M. Khan, S. Iqbal, M. A. Lodhi, Gh. M. Maharvi, Zia-Ullah, M. I. Choudhary, Attar-Rahmana, Sh. Perveen, *Bioorg. Med. Chem.* **2004**, 12, 1963; c) K. Niknam, A. Jamali, *Chin. J. Catal.* **2012**, 33, 1840.
- [60] a) A. Khazaei, F. Abbasi, A. R. Moosavi-Zare, *RSC Adv.* **2014**, 4, 1388. b) H. R. Shaterian, A. Hosseinian, M. Ghashang, *Tetrahedron Lett.* **2008**, 49, 5804.
- [61] K. Tabatabaeian, H. Heidari, A. Khorshidi, M. Mamaghani, N. O. Mahmoodi, *J. Serb. Chem. Soc.* **2011**, 76, 1.
- [62] R. Karimian, F. Piri, A. A. Safari, S. J. Davarpanah, *J. Nanostruct. Chem.* **2013**, 3, 52.
- [63] H. Mehrabi, H. Abusaidi, *J. Iran. Chem. Soc.* **2010**, 7, 890.
- [64] a) N. Koukabi, E. Kolvari, A. Khazaei, M. A. Zolfigol, B. Shirmardi-Shaghasemi, H. R. Khavasi, *Chem. Commun.* **2011**, 47, 9230. b) S. Qu, H. Yang, D. Ren, S. Kan, G. Zou, D. Liand, M. Li, *J. Colloid Interface Sci.* **1999**, 215, 190.
- [65] Y. H. Deng, C. C. Wang, J. H. Hu, W. L. Yang, S. K. Fu, *Colloids Surf. A* **2005**, 262, 87.

Supporting Information

Additional supporting information may be found in the online version of this article at the publisher's web site.